Published in final edited form as:
Biomaterials. 2010 December ; 31(35): 9293–9300. doi:10.1016/j.biomaterials.2010.08.041.

The use of BMP-2 coupled – Nanosilver-PLGA composite grafts to induce bone repair in grossly infected segmental defects

Zhong Zheng[a,1], **Wei Yin**[b,c,1], **Janette N. Zara**[d], **Weiming Li**[b,e], **Jinny Kwak**[b], **Rachna Mamidi**[f], **Min Lee**[d], **Ronald K. Siu**[b,d], **Richard Ngo**[g], **Joyce Wang**[h], **Doug Carpenter**[i], **Xinli Zhang**[b], **Benjamin Wu**[b,d,j], **Kang Ting**[b,**], and **Chia Soo**[a,*]

[a] Department of Orthopaedic Surgery, David Geffen School of Medicine, University of California, Los Angeles, CA 90095-1759, United States

[b] Department of Craniofacial Research Institute, University of California, Los Angeles, Los Angeles, CA 90095, United States

[c] Department of Endodontics & Periodontics, College of Stomatology, Dalian Medical University, Dalian, Liaoning 116044, PR China

[d] Department of Bioengineering, University of California, Los Angeles, Los Angeles, CA 90095, United States

[e] Department of Orthopaedics, the First Clinical Hospital of Harbin Medical University, Harbin, Heilongjiang 150081, PR China

[f] Department of Biochemistry, University of California, Los Angeles, Los Angeles, CA 90095, United States

[g] Department of Molecular, Cell and Developmental Biology, Los Angeles, Los Angeles, CA 90095, United States

[h] School of Medicine, University at Buffalo, Buffalo, NY 14260, United States

[i] QuantumSphere, Inc., Santa Ana, CA 92705, United States

[j] Department of Materials Science and Engineering, University of California, Los Angeles, Los Angeles, CA 90095, United States

Abstract

Healing of contaminated/infected bone defects is a significant clinical challenge. Prevalence of multi-antibiotic resistant organisms has renewed interest in the use of antiseptic silver as an effective, but less toxic antimicrobial with decreased potential for bacterial resistance. In this study, we demonstrated that metallic nanosilver particles (with a size of 20–40 nm)-poly(lactic-*co*-glycolic acid) (PLGA) composite grafts have strong antibacterial properties. In addition, nanosilver particles-PLGA composite grafts did not inhibit adherence, proliferation, alkaline phosphatase activity, or mineralization of ongrowth MC3T3-E1 pre-osteoblasts compared to PLGA controls. Furthermore, nanosilver particles did not affect the osteoinductivity of bone morphogenetic protein 2 (BMP-2). Infected femoral defects implanted with BMP-2 coupled 2.0% nanosilver particles-PLGA composite grafts healed in 12 weeks without evidence of residual

[*]Corresponding author. University of California, Los Angeles, David Geffen School of Medicine, Department of Orthopaedic Surgery, MRL 2641, Box 951759, 675 Charles E Young Drive, South, Los Angeles, CA 90095-1759, United States. Fax: +1 310 206 7783.
[**]Corresponding author. bsoo@ucla.edu (C. Soo).
[1]These contributed equally to this study.

Disclosure
Dr. D. Carpenter is inventor on non-chemically based processing nanosilver patent (QSI-Nano® Silver; USPTO 7,282,167).

bacteria. In contrast, BMP-2 coupled PLGA control grafts failed to heal in the presence of continued bacterial colonies. Our results indicate that nanosilver of defined particle size is bactericidal without discernable *in vitro* and *in vivo* cytotoxicity or negative effects on BMP-2 osteoinductivity, making it an ideal antimicrobial for bone regeneration in infected wounds.

Keywords

Bone repair; Antimicrobial; Nanosilver particle; Bone morphogenetic protein 2 (BMP-2)

1. Introduction

Healing of contaminated/infected bone defects is in essence a “race” between infectious organisms that seek to contaminate, colonize, and ultimately infect the implanted bone graft versus the body’s own endogenous tissues that seek to grow into the osseous defect via osteogenesis and neovascularization in the formation of a functional bony union. The need for bone grafts to repair significant bone loss in a non-sterile wound poses an additional challenge as the bone graft can serve as a nidus for infection. In fact, implantation of bone graft materials such as autograft bone or allograft is contra-indicated in actively infected wounds [1,2]. Bone graft infections are devastating complications requiring multiple debridement surgeries, local antibiotic bead implantation, and long-term systemic antibiotic treatment to eradicate infection prior to reconstructive re-grafting attempts [1,3]. This leads to significant medical costs for surgeries, antibiotic therapy, and lost productivity as well as major patient morbidity related to multiple surgeries, adverse antibiotic reactions, development of multi-resistant bacteria, and decreased quality of life [4]. Therefore, it would be advantageous to have tissue engineered bone graft devices that simultaneously control infection while promoting bone regeneration in order to avoid multiple surgeries and delayed reconstruction.

Bone repair is a highly concerted process involving osteogenic stem cells, osteoconductive surfaces, and osteoinductive growth factors that are severely disrupted by bacterial toxins and host inflammatory responses–thus, controlling infection is a key factor in successful regeneration in non-sterile bone defects. Creation of a favorable microenvironment for bone repair in this clinical setting would require a resorbable, biocompatible bone graft device with osteoinductive, osteoconductive, and antimicrobial properties. Although there are many advantages to using autologous graft, major drawbacks to this strategy include the extra surgery time for harvesting autologous bone, morbidity at the donor site including post-operative pain, hypersensitivity, pelvic instability, paresthesia, and infection [5–7], as well as limited availability of bone at the donor site. Meanwhile, allogeneic grafts can introduce infection risks and are less effective than autograft bone. Therefore, synthetic materials that are simultaneously osteoinductive and antimicrobial are potentially better therapeutic adjuncts for infected wounds. Poly(lactic-*co*-glycolic acid) (PLGA) has been used for decades in clinical applications, including prosthetic devices, implants [8], and microspheres for drug delivery [9,10] because it is a USA Food and Drug Administration (FDA)-approved biodegradable and biocom-patible polymer [9], that can be manufactured as a porous material with various surface textures. Meanwhile, bone morphogenetic protein 2 (BMP-2) is a proven strong osteoinductive factor, and used for the treatment of many bone fractures and bone defects [8,11,12]. Therefore, the combination of a BMP-2 coupled PLGA graft has potential to be an ideal clinically applicable bone scaffold.

Current antimicrobials used locally in bone graft infections are antibiotics, which generally bind to specific chemical targets that exist in bacteria but not in humans [13]. However, this binding specificity for a given antibiotic also narrows the number of bacterial species and

strains that are susceptible to a given antibiotic, and contributes significantly to the development of antibiotic resistance [14]. This issue is made more serious by the increasing number of infections caused by multi-drug resistant bacteria [15], prompting a search for antimicrobial alternatives. For example, gentamicin is the most frequently used antibiotic in bone tissue engineering due to its relatively minimal cytotoxic effects with local implantation [16]. However, during the last decade, there has been an increase in the number of deep periprosthetic infections caused by resistant bacteria, such as methicillin-resistant *Staphylococcus aureus* (MRSA) or methicillin-resistant *Staphylococcus epidermidis* (MRSE) [15,17–19], with several of them exhibiting multi-antibiotic drug resistance [20].

Silver, an antiseptic targeting a broad spectrum of $Gram^+$ and $Gram^-$ bacteria such as MRSE, MRSA and even vancomycin-resistant strains [14,20–22], has been used in different fields of medicine for years [23–28]. By binding and disrupting multiple components of bacterial structure/metabolism [23,29], silver is less likely to promote bacterial resistance than antibiotics. Bacterial resistance to silver [30] requires at least three separate mutations in three different bacterial systems–all within one generation of bacteria [23], and so far silver-resistant bacteria do not play a major role in hospital microbial germ flora [20]. Owing to advances in nano-technology, it is now possible to produce pure silver particles at the nanoscale. The advantage of nanoparticles is their greater surface to mass ratio. Thus, nanosilver particles offer greater solubility and chemical reactivity, and higher antibacterial activity compared to conventional silver preparations [21,22]. The purpose of this study was to create BMP-2 coupled nanosilver-PLGA composite (BMP-2/NS/PLGA) bone grafts as infected bone segmental defect adjunctive therapy. Antibacterial activity against bacteria and cytotoxicity of nanosilver coupled BMP-2/NS/PLGA grafts were studied *in vitro* and *in vivo*. Furthermore, an infected femoral defect model was utilized to evaluate the efficacy of BMP-2/NS/PLGA bone graft *in vivo*.

2. Materials and methods

2.1. Nanosilver

Nanosilver used in this study is in 20–40 nm silver particle form (QSI-Nano® Silver) obtained from QuantumSphere, Inc. (Santa Ana, CA).

2.2. Bone graft

Bone grafts were manufactured using a combination of published leaching techniques [31,32]. Briefly, the desired amount of nanosilver was mixed thoroughly with 17.5% (w/v) PLGA [85:15 poly(DL-lactic-*co*-glycolic acid), inherent viscosity: 0.64 dl/g in chloroform; Durect Co., Pelham, AL]-chloroform solution. The concentration of silver refers to the weight ratio of nanosilver mixed with PLGA. This solution was then poured onto a bed of sieved sugar particles with a size of 200–300 μm to generate a homogenous paste (Supplemental Fig. 1a), which was then stacked into a Teflon mold (Supplemental Fig. 1b) to generate 4 mm diameter ×7 mm length cylindrical grafts (Supplemental Fig.1c). The grafts were placed in a chemical hood for 12 h and lyophilized for 4 h, followed by repeated washing with large amounts of distilled water to leach the sugar. After the sugar-leaching process, the microporous grafts were air dried, sterilized in 70% alcohol and air dried again in a biosafety cabinet. The surface morphology of the grafts was evaluated using scanning electron microscopy (SEM, JEOL JSM-6700, Tokyo, Japan) [33]. Prior to SEM analysis, the samples were mounted on aluminum stubs and carbon coated. In addition, for *in vitro* cytotoxicity assay and *in vivo* animal model studies, 30 μg/ml BMP-2 in a total volume of 75 μl was injected into the graft and lyophilized to create a BMP-2/NS/PLGA bone graft.

2.3. In vitro antimicrobial activity

Vancomycin-resistant MRSA clinical strain *S. aureus* Mu50 (ATCC 700699) was used in a bacterial infection model. *In vitro* testing of the antimicrobial activity of the different doses of nanosilver was done using a microplate proliferation assay [20,34]. Specifically, the grafts were incubated with 10^7 or 10^8 bacterial colony forming units (CFU) in 200 μl of brain heart infusion broth (BHIB; BD, Sparks, MD) in each well of a 96-well microplate (Corning Inc., Corning, NY) at 37 °C for 1 h to allow adherence of the microorganisms to the graft surface. After incubation, grafts were rinsed with phosphate buffered saline (PBS) to remove loosely attached surface cells, and then incubated in 200 μl PBS with 0.25% glucose, 0.2% $(NH_4)_2SO_4$, and 1% sterile BHIB for 18 h at 37 °C in another 96-well microplate. During this second incubation step, the viable bacteria attached to the surface or within the grafts start to multiply and to release colonial counterparts into the well. After removal of the grafts, 100 μl released bacteria were transferred into another 96-well microplate and then amplified by adding 100 μl fresh BHIB for another 40 h at 37 °C. Proliferation of the released daughter cells were monitored at a wavelength of 595 nm online by Tecan Infinite f200 microplate reader (Tecan, Durham, NC) to generate a time-proliferation curve for each well of the microplate. If bacteria were partially or completely inactivated by the graft, they were able to seed only a few or even no daughter cells resulting in lagging or absence of bacterial growth [20]. In addition, general *S. aureus* strain SA113 (ATCC 35556) was also evaluated.

2.4. In vitro cytotoxicity testing

Passage 18 mouse pre-osteoblastic MC3T3-E1 cell line (subclone 4, ATCC CRL-2593) was employed for *in vitro* cytotoxicity evaluation of nanosilver-PLGA composite (NS/PLGA) grafts. MC3T3-E1 cells were maintained in α-minimal essential medium (α-MEM) supplied with 10% fetal bovine serum (FBS), 1% HT supplement, 100 units/ml penicillin and 100 μg/ml streptomycin (maintenance medium) at 37 °C with 5% CO_2. Five thousand cells were seeded on the bone grafts for testing. All media for cell culture were purchased from Gibco (Invitrogen, Calsbad, CA). Cell viability was estimated by 3-(4,5-dimethylthiazol-2-yl)-2,5-diphenyltetrazolium bromide (MTT) metabolism using commercially available Vybrand® MTT Cell Proliferation Assay Kit (Molecular Probes, Invitrogen, Calsbad, CA) with Tecan Infinite f200 microplate reader. In addition, after cultivation in osteoblastic differentiation medium (maintenance medium supplied with 50 μg/ml ascorbic acid and 10 mM β-glycerophosphate), alkaline phosphatase (ALP) activity and degree of mineralization (assessed by Alizarin Red staining) of MC3T3-E1 cells were also quantified [35,36].

2.5. Rat femoral segmental defect model

All surgical procedures were approved by the UCLA Chancellor's Animal Research Committee (2008-073). To standardize bone regeneration characteristics,16–18 week old male Sprague-Dawley (SD) rats were randomly divided into groups of eight. Animals were anesthetized by isoflurane inhalation. With use of aseptic technique, a 25–30 mm longitudinal incisionwas made over the anterolateral aspectof the femur. The femoral shaft was then exposed by separating the vastus lateralis and biceps femoris muscles. A polyethylene plate (length: 23 mm; width: 4 mm; height: 4 mm) was placed on the anterolateral surface of the femur. The plate contained six pre-drilled holes to accommodate 0.9 mm diameter threaded Kirschner wires. Taking the plate as a template, six threaded Kirschner wires were drilled through the plate and both cortices. With a small oscillating saw blade (Stryker, MI, USA), a 6-mm critical-sized mid-diaphyseal defect was created. The volume of the defect was approximately 75 μl. A bone graft injected with 10^8 CFU *S. aureus* Mu50 in 75 μl 20% gelatin gel was implanted into the defect. The overlying muscle and fascia were then closed with 4–0 Vicryl absorbable suture to secure the implant in place. Following surgery, the animals were housed in separate cages and allowed to eat and drink

ad libitum. Weight bearing was started immediately postoperatively, and animals were monitored daily. Bupre-norphine was administered for 2 days as an analgesic, but no antibiotic was administered.

2.6. Radiograph and three-dimensional micro-computerized tomography scanning

At 2, 4, 6, 8, 10, and 12 weeks post implantation, high-resolution lateral radiographs were obtained while the animals were under isoflurane sedation. Animals were euthanized at 12 weeks post implantation. The femurs were dissected, harvested, and fixed in 10% buffered formalin (Fisher Scientific, Fair Lawn, NJ). Following fixation for a minimum of 48 h, samples were scanned using high-resolution micro-computerized tomography (microCT; Skyscan 1172, Skyscan Belgium) at an image resolution of 16.1 μm (55 kVp and 181 μA radiation source with a 0.5 mm aluminum filter). 2D and 3D high-resolution reconstruction images were performed using the softwares provided by the manufacturer, and bone mineral density (BMD) and percent bone volume (BV/TV) were assessed to quantify newly formed bone bridge [37,38].

2.7. Histological and immunohistochemical evaluation

Following 3D microCT scanning, the specimen was decalcified using Cal-Ex solution (Fisher) for seven to nine days, washed with running tap water for 3–4 h and then transferred to a 75% ethanol solution, followed by embedding in paraffin. 5-μm sagittal sections of each specimen were obtained. Hematoxylin and eosin (H&E) and Masson's trichrome [39] staining were used for morphology estimation. Meanwhile, Taylor modified Brown and Brenn gram staining [40] was used to detect bacterial growth in the tissue. In addition, immunohistochemical (IHC) staining of osteocalcin (OCN) was also used for bone maturity evaluation [41,42].

2.8. Statistical analysis

The results were graphically depicted as the mean ±the standard deviation (SD). Two-tailed *t*-test and one-way ANOVA were performed (SPSS 13.0 for Windows, SPSS, Chicago, IL) to detect statistically significant differences. P value < 0.05 was considered statistically significant.

3. Results

3.1. Nanosilver coupled on PLGA bone graft

The microstructure of NS/PLGA grafts was analyzed by SEM. Aggregates or particles sintered together were not present in the silver (metal)-PLGA (polymer) composite grafts containing up to 2.0% silver (Fig. 1a–c). On the other hand, nanosilver particles aggregated in the composite grafts at higher silver concentrations (Fig. 1d). Because the bioactivity of silver is mostly based on generation and/or release of oxidative silver [14], asymmetric distribution of nanosilver particles will result in uneven local concentration of oxidative silver followed by variable local antibacterial activity and cytotoxicity. Therefore, the ceiling concentration of nanosilver in this study was established as 2.0%.

3.2. Antibacterial activity of nanosilver

Control PLGA grafts with no nanosilver did not inhibit proliferation of *S. aureus* Mu50 *in vitro*, while dose dependent bactericidal activity was observed in NS/PLGA grafts (Fig. 2). Grafts with 0.1% nanosilver did not affect 10^7 or 10^8 CFU *S. aureus* Mu50 proliferation, however, when the concentration of nanosilver was increased to 0.5%, bacterial proliferation was delayed in both inoculum densities. Higher concentrations at 1.0% and 1.5% NS/PLGA grafts were even more effective against *S. aureus* Mu50, completely inhibiting proliferation

of the lower inoculum of 10^7 CFU and retarding proliferation of 10^8 CFU. At the established ceiling concentration of 2.0% nanosilver, bacterial proliferation of up to 10^8 CFU was completely inhibited *in vitro* (Fig. 2).

In addition, our studies on another strain *S. aureus* SA113, wildly used as a model for virulence [43,44] exhibited the following: (1) 0.1% nanosilver-PLGA composite grafts delayed *S. aureus* SA113 proliferation at 10^6 CFU inoculation, while proliferation was completely inhibited by grafts with 0.5–2.0% nanosilver at the same condition; and (2) 2.0% NS/PLGA grafts completely inhibited *S. aureus* SA113 proliferation of as high as 10^{12} CFU inoculation (Supplemental Fig. 2).

Similar to the *in vitro* studies described above, 10^8 CFU *S. aureus* Mu50 induced continuous infection in a rat femoral segmental defect model with control PLGA graft implantation *in vivo* (Fig. 3a), while grafts with 1.0% nanosilver significantly reduced *S. aureus* Mu50 survival (Fig. 3b). Phagocytes were the predominant cells found in grafts with 0.0% and 1.0% nanosilver (Fig. 3a and b). On the other hand, only limited bacterial colonies were observed in 2.0% NS/PLGA grafts *in vivo*, and more red blood cells were found in the grafts instead of phagocytes at 2 weeks post implantation (Fig. 3c).

3.3. Cytotoxicity

Mouse pre-osteoblastic MC3T3-E1 cells grew into the grafts in both maintenance and osteoblastic differentiation medium (Fig. 4). Neither BMP-2 nor up to 2.0% nanosilver affected the viability of MC3T3-E1 cells in maintenance medium (Fig. 4a and b). Interestingly, 1.0% nanosilver led to more ongrowth MC3T3-E1 cell proliferation (Fig. 4c and d) as well as their ALP activity (Fig. 4e) in osteoblastic differentiation medium. In addition, no significant difference was found in qualitative mineralization evaluation between the BMP-2/NS/PLGA bone grafts and the non-toxic control group (BMP-2/PLGA bone grafts) *in vitro* (Fig. 4f).

Furthermore, *in vivo* studies also revealed that bone regenerated on BMP-2/NS/PLGA bone grafts as well as it did in uncontaminated rat femoral defect controls, indicating good biocompatibility of BMP-2/NS/PLGA grafts (Supplemental Fig. 3).

3.4. Implantation of BMP-2/NS/PLGA bone graft in infected critical femoral segmental defects

3.4.1. Radiography—Radiographic images showed none or extremely limited bone regeneration in *S. aureus* Mu50 contaminated defects implanted with control BMP-2/PLGA grafts and BMP-2/1.0% NS/PLGA grafts, respectively, up to 12 weeks post implantation (Fig. 5). In addition, there was a loss of bone within the femoral shaft with regression of the proximal and distal cut ends, and significant ectopic bone formation observed in the control group. On the contrary, as early as 6 weeks post implantation, defect fusion resulting from new bone formation was observed in 60% of animals in the group implanted with BMP-2/2.0% NS/PLGA grafts (Fig. 5). Radiographic findings of bone formation in the femurs were also confirmed by 3D microCT analysis (Supplemental Fig. 4). 3D reconstruction images from the microCT scan exhibited fusion in the BMP-2/2.0% NS/PLGA group, paralleling the quantitative data as well as the 2D radiographic results. In addition, bone mineral density (BMD, $P < 0.04$) and percent bone volume (BV/TV, $P < 0.05$) were found to be significantly greater in the BMP-2/2.0% NS/PLGA group compared to the BMP-2/PLGA control group.

3.4.2. Histological and IHC analysis—The quality of newly formed bone was further evaluated by H&E and Masson's trichrome staining, while Taylor modified Brown and

Brenn gram staining was employed to identify bacterial residue. Consistent with radiographic analyses, there was minimal evidence of bone regeneration with absence of a bony bridge formation in the contaminated femur defect area implanted with BMP-2/PLGA control grafts (Fig. 6a and b) or BMP-2/1.0% NS/PLGA grafts (Fig. 6d and e) after 12 weeks. However, despite continued bacterial contamination observed, the number of bacterial colonies was reduced in both groups at 12 weeks (Fig. 6c and f) compared to tissues harvested after 2 weeks post implantation. In contrast, no *S. aureus* Mu50 survival was evident in the contaminated femurs implanted with BMP-2/2.0% NS/PLGA bone grafts after 12 weeks (Fig. 6i). By eliminating bacteria in the defect, BMP-2/2.0% NS/PLGA grafts promoted significantly more bone formation compared to the control group (Fig. 6g and h, Supplemental Fig. 4). Furthermore, a mineralized bony bridge connecting the two defect ends was clearly identified by both Masson's trichrome staining and OCN IHC staining (Fig. 6h and j). High intensity OCN signals signify that new bone formation was still active in the defect area, especially around the mineralized bridge and in the marrow-like cavities (Fig. 6j–j2) at 12 weeks post implantation.

4. Discussion

Infection of bone graft devices is considered a devastating complication. The major critical barrier to progress is the absence of an integrated approach to infection control and bone regeneration for the bone graft device. Clinically, bone graft devices implanted into infected wounds need to prevent bacterial infection while promoting cellular ingrowth. Although the ability of antibiotics to bind specific bacterial chemical targets desirably limits their toxicity, it also narrows the susceptibility of bacterial species and strains to a given antibiotic–and contributes significantly to development of multi-drug resistant bacteria [14]. In contrast, antiseptics such as silver are broad spectrum agents that are less likely to promote bacterial resistance because silver non-selectively targets many cellular processes [14,23,45].

Silver has been used for centuries in water recycling and sanitization and for treatment of wound infections due to its broad antibacterial spectrum [23,30]. With the development of modern antibiotics, silver use for infection control declined significantly. However, beginning in the late 1960s, silver experienced wide use as an antimicrobial in cutaneous wounds [23]. Modern uses of silver include a variety of silver-based dressings in the form of creams, foams, hydrogels, hydrocolloids, polymeric films, and meshes [23]. In addition, silver is used to reduce bacterial colonization/infection in a broad range of devices such as vascular and urinary catheters, endotracheal tubes, and implantable prostheses [24,25]. In the orthopaedic area, electrically generated silver ions have been successfully used to treat chronic osteomyelitis and infected non-unions [26–28]. Mechanistically, silver-based antimicrobials are thought to attach to specific thiol groups containing sulfur and hydrogen found in a variety of structural and functional bacterial proteins; however, they may differ in the reservoir form for the active silver [14]. Ionic reservoir form of silver, such as silver nitrate ($AgNO_3$) and silver sulfate (Ag_2SO_4), were previously used to protect against bacterial infection [30,46,47]. However, inadequate local retention and severe cytotoxic effects limited the clinical use of ionic silver for bone grafts despite its good short-term antibacterial activity [46–48]. Fortunately, recent developments in nano-technology have made the creation of new biomedical materials possible, including generation of nanosilver particles. Compared to non-nanoscale silver, nanosilver particles provide a larger surface area to interface with the environment. Previous studies have demonstrated that 5–50 nm size nanosilver particles are bactericidal [20]. Further investigation suggested that the greater the surface area of nanosilver particle the greater the antibacterial activity [22,49–52]. However, the nanosilver particles used are commonly synthesized through chemical reduction of a silver salt solution by a reducing agent, leading to residual chemical impurities and wide distribution of particle sizes that can confound interpretation of the

antibacterial performance of nanosilver particles [22,53]. To minimize this, highly purified (>99.9% pure), 20–40 nm nanosilver particles produced through a novel, non-chemically based, proprietary process (QSI-Nano® Silver; USPTO 7,282,167) were used in this study. The active surface of QSI-Nano® Silver (15–25 m^2/g) is much greater compared to commercial non-nanoscale silver powder (1–2 m^2/g) and previously *in vitro* studied nanosilver particles (4 m^2/g, [20]), which suggests that QSI-Nano® Silver may have better antibacterial activity. In this study, we demonstrated that NS/PLGA grafts have excellent antibacterial activity against proliferation of *S. aureus*, which is the bacterial pathogen responsible for ~80% of all cases of human osteomyelitis [54]. The absence of *in vitro* and *in vivo* cytotoxicity of NS/PLGA bone grafts was also shown. Thus, an NS/PLGA graft is particularly promising for use in bone regeneration of contaminated wounds due to its potential effectiveness against multi-drug resistant bacteria that cannot be achieved by available antibiotic agents.

In the creation of a BMP-2/NS/PLGA composite graft, the effect of nanosilver particle on BMP-2 was also considered, as nanosilver particles could possibly interfere with essential cellular elements relating to BMP-2 osteoinductivity when it binds to thiol groups. Fortunately, up to 2.0% concentration of nanosilver particles did not interrupt bone regeneration induced by BMP-2 either *in vitro* or *in vivo* as shown in this study. Not surprisingly, infected defects healed slower compared to non-infected defects, although much faster than infected controls treated without nanosilver. The slower healing time could be attributed to partial BMP-2 loss and depletion by bacteria so that the actual BMP-2 dose is effectively decreased in an infected defect compared to a non-infected one. Future studies using an alternative system for controlled BMP-2 delivery and release, such as via microsphere [33], should be considered to overcome this problem.

In summary, employing nanosilver particles, we have successfully regenerated bone in a 6-mm critical-sized defect (total volume ~75 μl) infected with 10^8 CFU vancomycin-resistant MRSA strain Mu50 (i.e., ~10^9 CFU/ml bacteria, which far exceeds the typical 10^5 CFU/ml criteria for invasive tissue infection [55]).

5. Conclusions

In this study, BMP-2/NS/PLGA composite grafts exhibited significant antibacterial and osteoinductive activity. Our results demonstrated that nanosilver is an effective antimicrobial that is non-toxic, and does not interfere with BMP-2 induced bone formation. In addition, our results also showed that the efficacy of nanosilver is dose dependent, raising the possibility that by using surfactant to minimize NS aggregation, we can fabricate BMP-2/NS/PLGA scaffolds with even higher silver concentrations than the present 2% NS to provide even more potent antibacterial activity.

Supplementary Material

Refer to Web version on PubMed Central for supplementary material.

Acknowledgments

This research was supported by US DoD Grant 07128099. The authors would like to thank Dr. Michael Chiang from the Department of Craniofacial Research Institute, University of California, Los Angeles for assisting in microCT scanning and analysis.

References

1. Farooq AH, Dabke HV, Majeed MA, Carbarns NJ, Mackie IG. Clostridial wound infection following reconstruction of the anterior cruciate ligament using bone-patella-bone autograft. J Coll Physicians Surg Pak. 2007; 17:369–70. [PubMed: 17623592]
2. Journeaux SF, Johnson N, Bryce SL, Friedman SJ, Sommerville SM, Morgan DA. Bacterial contamination rates during bone allograft retrieval. J Arthroplasty. 1999; 14:677–81. [PubMed: 10512439]
3. Bruce JN, Bruce SS. Preservation of bone flaps in patients with postcraniotomy infections. J Neurosurg. 2003; 98:1203–7. [PubMed: 12816265]
4. Mader JT, Shirtliff ME, Bergquist SC, Calhoun J. Antimicrobial treatment of chronic osteomyelitis. Clin Orthop Relat Res. 1999; 360:47–65. [PubMed: 10101310]
5. Lane JM, Tomin E, Bostrom MP. Biosynthetic bone grafting. Clin Orthop Relat Res. 1999; 367:S107–17. [PubMed: 10546640]
6. Arrington ED, Smith WJ, Chambers HG, Bucknell AL, Davino NA. Complications of iliac crest bone graft harvesting. Clin Orthop Relat Res. 1996; 329:300–9. [PubMed: 8769465]
7. Damien CJ, Parsons JR. Bone graft and bone graft substitutes: a review of current technology and applications. J Appl Biomater. 1991; 2:187–208. [PubMed: 10149083]
8. Yu D, Li Q, Mu X, Chang T, Xiong Z. Bone regeneration of critical calvarial defect in goat model by PLGA/TCP/rhBMP-2 scaffolds prepared by low-temperature rapid-prototyping technology. Int J Oral Maxillofac Surg. 2008; 37:929–34. [PubMed: 18768295]
9. Jain RA. The manufacturing techniques of various drug loaded biodegradable poly(lactide-*co*-glycolide) (PLGA) devices. Biomaterials. 2000; 21:2475–90. [PubMed: 11055295]
10. Putney SD, Burke PA. Improving protein therapeutics with sustained-release formulations. Nat Biotechnol. 1998; 16:153–7. [PubMed: 9487521]
11. Kang Q, Sun MH, Cheng H, Peng Y, Montag AG, Deyrup AT, et al. Characterization of the distinct orthotopic bone-forming activity of 14 BMPs using recombinant adenovirus-mediated gene delivery. Gene Ther. 2004; 11:1312–20. [PubMed: 15269709]
12. Govender S, Csimma C, Genant HK, Valentin-Opran A, Amit Y, Arbel R, et al. Recombinant human bone morphogenetic protein-2 for treatment of open tibial fractures: a prospective, controlled, randomized study of four hundred and fifty patients. J Bone Joint Surg Am. 2002; 84:2123–34. [PubMed: 12473698]
13. Van de Belt H, Neut D, Schenk W, van Horn JR, van der Mei HC, Busscher HJ. Infection of orthopedic implants and the use of antibiotic-loaded bone cements. A review. Acta Orthop Scand. 2001; 72:557–71. [PubMed: 11817870]
14. Ovington LG. The truth about silver. Ostomy Wound Manage. 2004; 50:1S–10S. [PubMed: 15499162]
15. Kilgus DJ, Howe DJ, Strang A. Results of periprosthetic hip and knee infections caused by resistant bacteria. Clin Orthop Relat Res. 2002; 404:116–24. [PubMed: 12439249]
16. Josefsson G, Kolmert L. Prophylaxis with systematic antibiotics versus gentamicin bone cement in total hip arthroplasty. A ten-year survey of 1,688 hips. Clin Orthop Relat Res. 1993; 292:210–4. [PubMed: 8519111]
17. Hirakawa K, Stulberg BN, Wilde AH, Bauer TW, Secic M. Results of 2-stage reimplantation for infected total knee arthroplasty. J Arthroplasty. 1998; 13:22–8. [PubMed: 9493534]
18. James PJ, Butcher IA, Gardner ER, Hamblen DL. Methicillin-resistant *Staphylococcus epidermidis* in infection of hip arthroplasties. J Bone Joint Surg Br. 1994; 76:725–7. [PubMed: 8083259]
19. Hope PG, Kristinsson KG, Norman P, Elson RA. Deep infection of cemented total hip arthroplasties caused by coagulase-negative staphylococci. J Bone Joint Surg Br. 1989; 71:851–5. [PubMed: 2584258]
20. Alt V, Bechert T, Steinrucke P, Wagener M, Seidel P, Dingeldein E, et al. An in vitro assessment of the antibacterial properties and cytotoxicity of nano-particulate silver bone cement. Biomaterials. 2004; 25:4383–91. [PubMed: 15046929]
21. Lok CN, Ho CM, Chen R, He QY, Yu WY, Sun H, et al. Silver nanoparticles: partial oxidation and antibacterial activities. J Biol Inorg Chem. 2007; 12:527–34. [PubMed: 17353996]

22. Martinez-Castanon GA, Nino-Martinez N, Martinez-Gutierrez F, Martinez-Mendoza JR, Ruiz F. Synthesis and antibacterial activity of silver nanoparticles with different sizes. J Nanopart Res. 2008; 10:1343–8.
23. Leaper DJ. Silver dressings: their role in wound management. Int Wound J. 2006; 3:282–94. [PubMed: 17199764]
24. Seymour C. Audit of catheter-associated UTI using silver alloy-coated foley catheters. Br J Nurs. 2006; 15:598–603. [PubMed: 16835528]
25. Hardes J, Ahrens H, Gebert C, Streitbuerger A, Buerger H, Erren M, et al. Lack of toxicological side-effects in silver-coated megaprostheses in humans. Biomaterials. 2007; 28:2869–75. [PubMed: 17368533]
26. Tamura K. Some effects of weak direct current and silver ions on experimental osteomyelitis and their clinical application. Nippon Seikeigeka Gakkai Zasshi. 1983; 57:187–97. [PubMed: 6602192]
27. Webster DA, Spadaro JA, Becker RO, Kramer S. Silver anode treatment of chronic osteomyelitis. Clin Orthop Relat Res. 1981; 161:105–14. [PubMed: 6975686]
28. Nand S, Sengar GK, Jain VK, Gupta TD. Dual use of silver for management of chronic bone infections and infected non-unions. J Indian Med Assoc. 1996; 94:91–5. [PubMed: 8810203]
29. Schreurs WJ, Rosenberg H. Effect of silver ions on transport and retention of phosphate by *Escherichia coli*. J Bacteriol. 1982; 152:7–13. [PubMed: 6749823]
30. Silver S, Phung le T, Silver G. Silver as biocides in burn and wound dressings and bacterial resistance to silver compounds. J Ind Microbiol Biotechnol. 2006; 33:627–34. [PubMed: 16761169]
31. Zheng Z, Deng Y, Lin XS, Zhang LX, Chen GQ. Induced production of rabbit articular cartilage-derived chondrocyte collagen II on polyhydroxyalkanoate blends. J Biomat Sci-Polym E. 2003; 14:615–24.
32. Deng Y, Lin XS, Zheng Z, Deng JG, Chen JC, Ma H, et al. Poly(hydroxybutyrate-co-hydroxyhexanoate) promoted production of extracellular matrix of articular cartilage chondrocytes in vitro. Biomaterials. 2003; 24:4273–81. [PubMed: 12853259]
33. Lee M, Li WM, Siu RK, Whang J, Zhang XL, Soo C, et al. Biomimetic apatite-coated alginate/chitosan microparticles as osteogenic protein carriers. Biomaterials. 2009; 30:6094–101. [PubMed: 19674782]
34. Bechert T, Steinrucke P, Guggenbichler JP. A new method for screening anti-infective biomaterials. Nat Med. 2000; 6:1053–6. [PubMed: 10973328]
35. Evangelista MB, Hsiong SX, Fernandes R, Sampaio P, Kong HJ, Barrias CC, et al. Upregulation of bone cell differentiation through immobilization within a synthetic extracellular matrix. Biomaterials. 2007; 28:3644–55. [PubMed: 17532040]
36. Gough JE, Jones JR, Hench LL. Nodule formation and mineralisation of human primary osteoblasts cultured on a porous bioactive glass scaffold. Biomaterials. 2004; 25:2039–46. [PubMed: 14741618]
37. Muller R, Ruegsegger P. Micro-tomographic imaging for the nondestructive evaluation of trabecular bone architecture. Stud Health Technol Inform. 1997; 40:61–79. [PubMed: 10168883]
38. Gauthier O, Muller R, von Stechow D, Lamy B, Weiss P, Bouler JM, et al. In vivo bone regeneration with injectable calcium phosphate biomaterial: a three-dimensional micro-computed tomographic, biomechanical and SEM study. Biomaterials. 2005; 26:5444–53. [PubMed: 15860201]
39. Foot NC. The Masson trichrome staining methods in routine laboratory use. Stain Technol. 1933; 8:101–10.
40. Taylor RD. Modification of Brown and Brenn gram stain for differential staining of gram-positive and gram-negative bacteria in tissue sections. Am J Clin Pathol. 1966; 46:472. [PubMed: 4162586]
41. Bobryshev YV, Killingsworth MC, Lord RSA. Spatial distribution of osteoblast-specific transcription factor Cbfa1 and bone formation in atherosclerotic arteries. Cell Tissue Res. 2008; 333:225–35. [PubMed: 18553107]

42. Kasai R, Bianco P, Robey PG, Kahn AJ. Production and characterization of an antibody against the human bone gla protein (Bgp/Osteocalcin) propeptide and its use in immunocytochemistry of bone-cells. Bone Miner. 1994; 25:167–82. [PubMed: 8086856]
43. Jonsson P, Lindberg M, Haraldsson I, Wadstrom T. Virulence of *Staphylococcus aureus* in a mouse mastitis model –studies of alpha-hemolysin, coagulase, and protein-A as possible virulence determinants with protoplast fusion and gene cloning. Infect Immun. 1985; 49:765–9. [PubMed: 4040889]
44. Peschel A, Jack RW, Otto M, Collins LV, Staubitz P, Nicholson G, et al. *Staphylococcus aureus* resistance to human defensins and evasion of neutrophil killing via the novel virulence factor MprF is based on modification of membrane lipids with L-lysine. J Exp Med. 2001; 193:1067–76. [PubMed: 11342591]
45. Gupta A, Phung LT, Taylor DE, Silver S. Diversity of silver resistance genes in IncH incompatibility group plasmids. Microbiology. 2001; 147:3393–402. [PubMed: 11739772]
46. Vik H, Andersen KJ, Julshamn K, Todnem K. Neuropathy caused by silver absorption from arthroplasty cement. Lancet. 1985; 1:872. [PubMed: 2858727]
47. Sudmann E, Vik H, Rait M, Todnem K, Andersen KJ, Julsham K, et al. Systemic and local silver accumulation after total hip replacement using silver-impregnated bone cement. Med Prog Technol. 1994; 20:179–84. [PubMed: 7877562]
48. Drewa T, Szmytkowska K, Chaberski M. The short term exposition of $AgNO_3$ on 3T3 mouse fibroblasts cell line. Acta Pol Pharm. 2007; 64:175–8. [PubMed: 17665868]
49. Jeong SH, Yeo SY, Yi SC. The effect of filler particle size on the antibacterial properties of compounded polymer/silver fibers. J Mater Sci. 2005; 40:5407–11.
50. Jeong SH, Hwang YH, Yi SC. Antibacterial properties of padded PP/PE nonwovens incorporating nano-sized silver colloids. J Mater Sci. 2005; 40:5413–8.
51. Thiel J, Pakstis L, Buzby S, Raffi M, Ni C, Pochan DJ, et al. Antibacterial properties of silver-doped titania. Small. 2007; 3:799–803. [PubMed: 17340662]
52. Martinez-Gutierrez F, Olive PL, Banuelos A, Orrantia E, Nino N, Sanchez EM, et al. Synthesis, characterization, and evaluation of antimicrobial and cytotoxic effect of silver and titanium nanoparticles. Nanomedicine: Nanotechnol Biol Med. 2010 [Epub ahead of print].
53. Panacek A, Kvitek L, Prucek R, Kolar M, Vecerova R, Pizurova N, et al. Silver colloid nanoparticles: synthesis, characterization, and their antibacterial activity. J Phys Chem B. 2006; 110:16248–53. [PubMed: 16913750]
54. Ellington JK, Harris M, Webb L, Smith B, Smith T, Tan K, et al. Intracellular *Staphylococcus aureus*. A mechanism for the indolence of osteomyelitis. J Bone Jt Surg Br. 2003; 85:918–21.
55. Calandra T, Cohen J, Infect ISFD. The international sepsis forum consensus conference on definitions of infection in the intensive care unit. Crit Care Med. 2005; 33:1538–48. [PubMed: 16003060]

Appendix

Figures with essential colour discrimination. Figs. 3 and 6 of this article has parts that are difficult to interpret in black and white. The full colour images can be found in the online version, at doi:10.1016/j.biomaterials.2010.08.041.

Appendix. Supplementary information

Supplementary information associated with this article can be found in the online version at doi:10.1016/j.biomaterials.2010.08. 041.

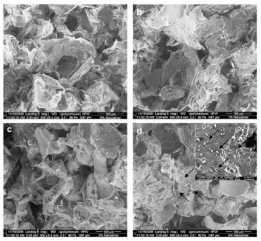

Fig. 1.

Scanning electron microscopy of bone grafts. Compared to control PLGA grafts (a), no significant difference was found in nanosilver-PLGA composite grafts with 1.0% (b) and 2.0% (c) nanosilver particles. However, particles aggregated (arrows) in the composite grafts with 5.0% nanosilver (d).

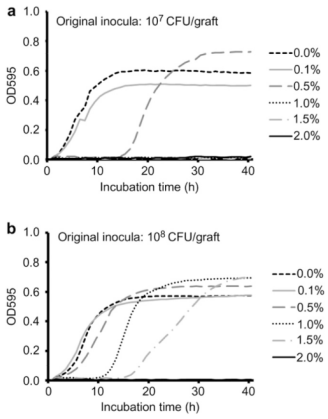

Fig. 2.

In vitro antibacterial activity of nanosilver particle-PLGA composite grafts. Different inocula (a, 10^7 CFU; b, 10^8 CFU) of *Staphylococcus aureus* Mu50 were injected for microplate proliferation assay.

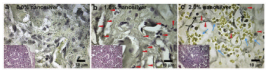

Fig. 3.

In vivo antibacterial activity of nanosilver particle-PLGA composite grafts. After 2-week contamination with 10^8 CFU *S. aureus* Mu50, rat femoral segmental defects with implanted grafts were harvested, fixed, decalcified, embedded, sectioned and stained with Taylor modified Brown and Brenn gram stain as well as H&E (insert figures). Compared to serious bacterial infection (black dots) found in control PLGA grafts (a), 1.0% nanosilver-PLGA composite grafts significantly reduced bacterial survival to colonized collation (b, red arrows). On the other hand, only limited bacterial colonies (red arrows) were observed in 2.0% nanosilver particle-PLGA composite grafts *in vivo* (c), and more red blood cells (blue arrows) were found in the grafts instead of phagocytes (black arrows).

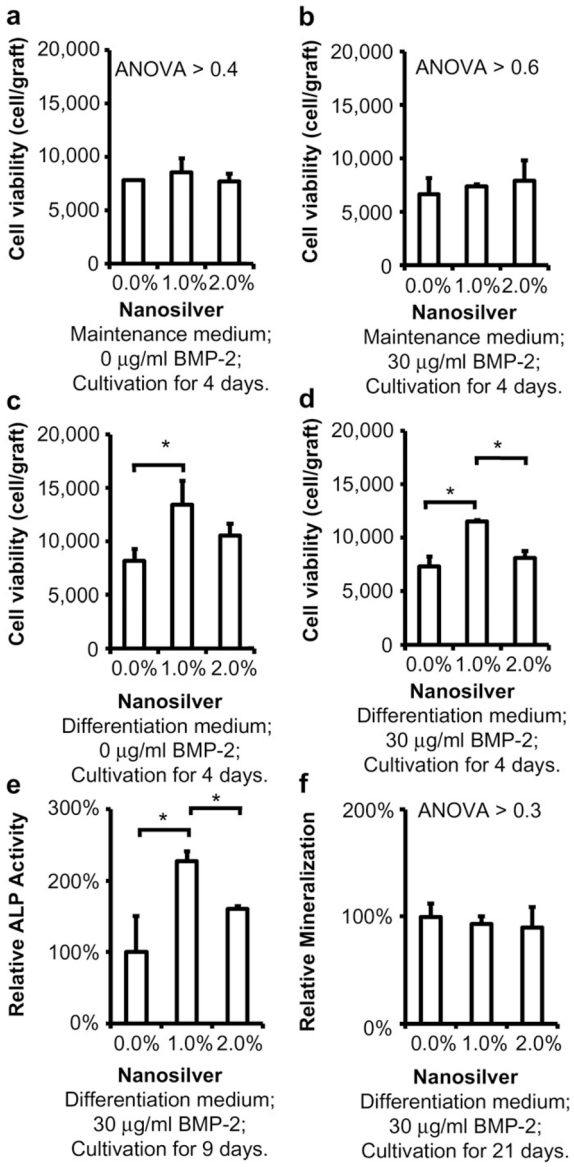

Fig. 4.

In vitro cytotoxicity of nanosilver particle-PLGA composite grafts. In maintenance medium, up to 2.0% nanosilver did not affect MC3T3-E1 viability with 0 (a) or 30 μg/ml (b) BMP-2. Interestingly, 1.0% nanosilver-PLGA composite grafts induced MC3T3-E1 proliferation in differentiation medium with 0 (c) or 30 μg/ml (d) BMP-2, as well as its ALP activity (e). Otherwise, no significant difference on mineralization was found between the tested grafts (f). *, $P < 0.05$; $N = 6$ for each test.

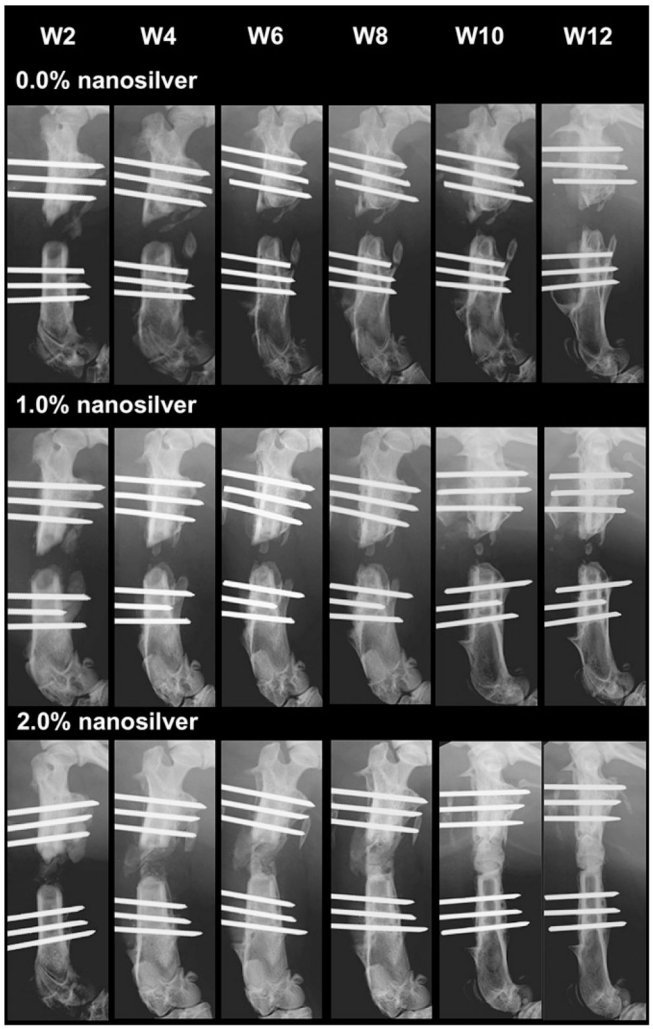

Fig. 5.

Radiographic images of 10^8 CFU *S. aureus* Mu50 infected rat femoral segmental defects implanted with 0.0% (a), 1.0% (b), and 2.0% (c) nanosilver-PLGA bone grafts coupled with 30 μg/ml BMP-2.

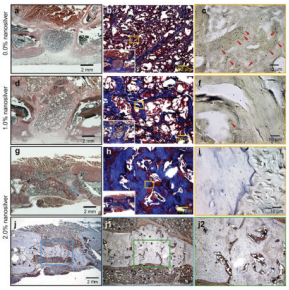

Fig. 6.

H&E staining (a, d, and g), Masson's trichrome staining (b, e, and h), Taylor modified Brown and Brenn gram stain (c, f, and i) and immunostaining of OCN (j, j1, and j2) of 10^8 CFU *S. aureus* Mu50 contaminated rat femoral segmental defects implanted with 0.0% (a–c), 1.0% (d–f), and 2.0% (g–j2) nanosilver-PLGA bone grafts coupled with 30 μg/ml BMP-2 at 12 weeks post implantation, respectively. Almost no bone regenerated in BMP-2/0.0%-NS/PLGA (control BMP-2 coupled control PLGA) implanted groups (a, and b) with obvious continued bacterial contamination (c, red arrows). Less bone regenerated in the defect area of BMP-2/1.0%-NS/PLGA implanted groups (d and e), while onlylimited bacterial colonies were observed (f, red arrow). BMP-2/2.0%-NS/PLGA grafts promoted significantly greater bone formation to form a mineralized bony bridge between the two defect ends (g, h, and j) by eliminating bacteria in the defect area (i), Higher magnification figures show active bone regeneration around the mineralized bridge and in the marrow-like cavities in the bridge (j1, and j2).